Non-Linear Steady-State Electrical Current Modeling for the Electropermeabilization of Biological Tissue

Marie Breton[1], Francois Buret[2], Laurent Krähenbühl[2], Michael Leguèbe[3], Lluis M. Mir[1], Ronan Perrussel[4], Clair Poignard[3], Riccardo Scorretti[2], and Damien Voyer[2]

[1]Team Vectorology and Anticancer Therapies, Institut Gustave Roussy, Villejuif Cedex F-94805, France
[2]École Centrale de Lyon, Université de Lyon, Lyon 69007, France
[3]Institut National de La Recherche en Informatique Appliquée de Bordeaux, Talence Cedex F-33405, France
[4]Laboratoire Plasma et Conversion d'Energie, Toulouse Cedex F-31071, France

We propose a non-linear steady-state model of irreversible electropermeabilization in a biological tissue. The non-linear problem is solved using a modified fixed point iteration. The unknown parameters are experimentally estimated from the observation of the necrosis on a potato tissue for different applied voltages. A variability study of the parameters involved in the model is performed.

***Index Terms*— Electropermeabilization (EP), non-linear conductivity.**

I. Introduction

THE membrane of a biological cell can become permeable when the cell is exposed to intense electric field pulses. This phenomenon discovered during the 1960s begins nowadays to be exploited in clinical applications, such as electrochemotherapy [1] and electrogenetherapy. The modeling of electropermeabilization (EP) is particulary complex because the changes in the membrane physiology induce at the cell scale (and therefore at the tissue scale) modifications of the conductivity that depend on the applied field. In [2], a first modeling of EP at the tissue scale is proposed, based on a phenomenological non-linear Ohm's law. This approach makes it possible to explain some quantitative experimental results. But, in this paper, we introduce a static sequential EP modeling in which the non-linear Ohm's law would explain the evolution of the EP. However, since there is no dynamic equation, the comparison between the numerical and experimental chronogramms of current is not convincing. In addition, the parameters of the model are estimated based on the current measured at the electrodes, which cannot provide any spatial information on the electropermeabilized region. In this paper, we propose to model the irreversible EP from the observation of the necrosis that appears when the EP reaches the irreversible threshold; the surface of the potato becomes darker and these experiments can be used to fit the parameters of the non-linear Ohm's law. Some uncertainties are introduced in our model (parameters in Ohm's law, position of the electrodes, and threshold defined to delimit the necrosis area) in order to identify the critical parameter(s) and quantify the uncertainty of the calculated necrosis surface [6].

II. Experiments

Potato samples of 1 cm^2 have been prepared as reported in [5] and electric pulses, with a rectangular shape and a duration of 50 ms, are applied for different voltages through electrodes separated by 7 mm. When the voltage exceeds a threshold, a dark region appears on the surface of the sample, indicating that irreversible EP has been reached. Indeed, the darkening is due to the necrosis or apoptosis. In order to obtain plentiful results, samples are put in a conductive gel made with agarose and sodium chloride [Fig. 2(d)] and three configurations are considered (Fig. 1): either both electrodes are dropped into the sample (case A), or one electrode is dropped into the sample and the other into the gel (cases B and C).

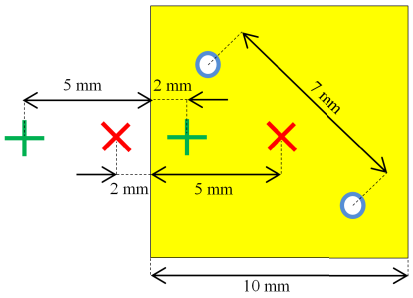

Fig. 1. Experimental setup. Spots represent the electrodes (o = case A, × = case B, + = case C).

For each case, nine experiments were performed with voltages spanning between 20 and 100 V by step of 10 V. A picture is taken one day after the application of pulses [Fig. 2(a)–(c)] since the darkening does not appear immediately. In order to distinguish the darkening due to EP to the one due to natural oxidation, a reference sample is prepared in the same conditions as the others (in particular, electrodes have been dropped in the same way) and no pulse was applied.

As one can expect, a dark region appears at the surface of the sample close to the electrode(s), and it grows as the voltage increases. In case A, the phenomenon is observed from 60 V, whereas it appears between 40 and 50 V in cases B and C because of the difference of conductivity between the gel and the potato. Besides, the shape of the necrosis region depends on the positioning of the electrodes.

Manuscript received May 25, 2014; accepted August 19, 2014. Date of current version April 22, 2015. Corresponding author: D. Voyer (e-mail: damien.voyer@ec-lyon.fr).

Color versions of one or more of the figures in this paper are available online at http://ieeexplore.ieee.org.

Digital Object Identifier 10.1109/TMAG.2014.2351836

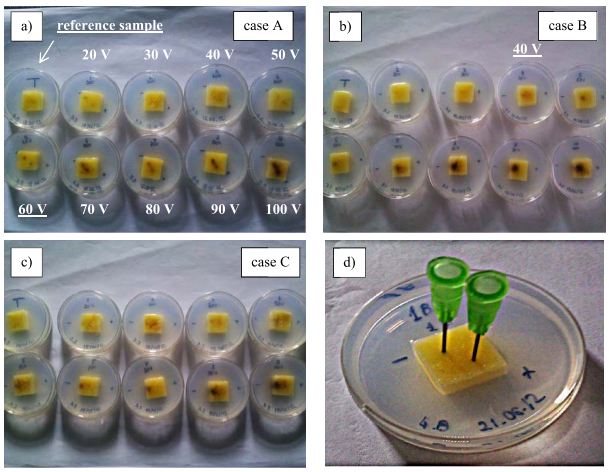

Fig. 2. (a)–(c) Picture of the samples (top left to bottom right: reference sample and samples with increasing voltages). (d) Experimental setup in case A.

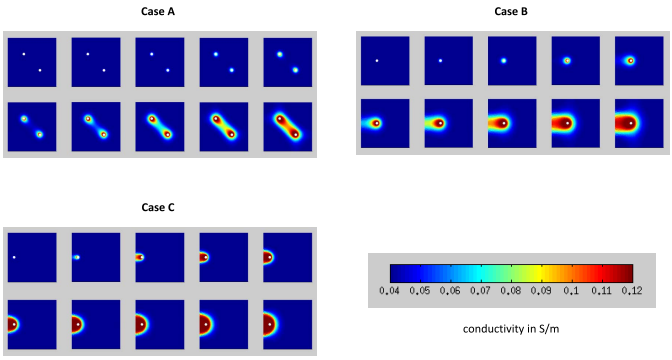

Fig. 3. Conductivity σ_{pot} computed for the same conditions as Fig. 2. The red region ($\sigma_{\text{pot}} \simeq \sigma_1$) corresponds to completely electropermeabilized tissue.

III. Modeling

A. Non-Linear Ohm's Law

Our model describes only the steady-state that appears once the process of EP is completed. While the conductivity of the gel σ_{gel} is constant, the conductivity of potato σ_{pot} is a non-linear function of the electric field and is modeled through a sigmoid function [2], [3]

$$\sigma_{\text{pot}}(\|\mathbf{E}\|) = \sigma_0 + \frac{\sigma_1 - \sigma_0}{2}[1 + \tanh(k(\|\mathbf{E}\| - E_{\text{thr}}))] \quad (1)$$

where $\mathbf{E} = -\text{grad}\, V$ is the electric field, σ_0 and σ_1 are, respectively, the conductivities for safe and electropermeabilized tissues, E_{thr} is a threshold electric field, and k is a fitting coefficient that modulates the transition to the EP. In [2], two thresholds of the electric field for reversible and irreversible EP are considered, but, in this paper, we define a single threshold for irreversible EP since reversible EP cannot be observed in our experiments. The problem is composed of the potato sample, the gel and the electrodes. It is ruled by a steady-state electric current equation with Neumann homogeneous boundary conditions on the outer boundary Γ_o and an imposed electric potential on the boundary of the electrodes Γ_e

$$\text{div}(\sigma\, \text{grad}\, V) = 0; \quad \mathbf{n} \cdot \text{grad}\, V|_{\Gamma_o} = 0; \quad V|_{\Gamma_e} = V_e. \quad (2)$$

B. Resolution of the Non-Linear Problem

Equation (2) is discretized in a 2-D domain by using the finite element method and this leads to a non-linear system

$$\mathbf{A}(\mathbf{v})\mathbf{v} = \mathbf{b} \quad (3)$$

which is solved numerically by using a modified fixed point iteration [4], that proves to be more efficient that the technique proposed in [2] (more details are given in the Appendix).

C. Estimation of the Unknown Parameters

In this problem, there are five unknown parameters: σ_0, σ_1, σ_{gel}, E_{thr}, and k. In [5], the conductivity for a safe potato has been measured by bioimpedancemetry and the estimated value is $\sigma_0 = 0.04$ S/m. When a tissue has undergone an irreversible EP, its conductivity increases by a factor of a few units since the membrane of cells is more permeable. As for the gel, its conductivity depends on the concentration of sodium chloride and it is higher than for safe potatoes. In the simulation presented hereafter, we set somehow arbitrarily: $\sigma_1 = 3\sigma_0$ and $\sigma_{\text{gel}} = 20\sigma_0$. A variability study (see Section III-E) shows that our model exhibits a moderate sensibility to these parameters. The electric threshold E_{thr} can be estimated more precisely; in the experiments case A, EP is observed close to the electrodes for applied voltages starting from 60 V. A simulation in which the conductivity of potato σ_{pot} is set to σ_0 allows computing the electric field in the neighborhood of the electrodes before EP occurs, which is a rather good estimate: $E_{\text{thr}} \simeq 115$ V/cm. Mind that the value of the electric field close to the electrodes depends strongly on the diameter of electrodes. Therefore, simulations must be performed with an accurate value of the diameter (0.8 mm in our experiments). The coefficient k modifies the sharpness for the transition between normal and EP conditions; we set arbitrarily: $k = 0.04$ cm/V, which leads to a rather smooth transition and yet the threshold is not too much underlined.

D. Comparison With Experiments

Simulations of cases A, B, and C have been carried out, and the distribution of the conductivity at the surface of the sample is shown in Fig. 3. The comparison with experiments is not trivial. In the region where cells have been electropermeabilized, oxidation occurs, and a dark region is observed experimentally. From an electrical point of view, the conductivity σ_{pot} in this area increased; therefore, it seems reasonable to compare the distribution of conductivity (Fig. 3) with the darkening (Fig. 2). However, passing from this qualitative statement to a quantitative one is a delicate issue, even in presence of a threshold effect. One observes that in our simulations, a electropermeabilized region appears for an applied voltage of $\sim$60 V in case A, 40 V in case B, and even earlier in case C; these observations agree rather well with our experimental results. In addition, the shape of the dark regions is close

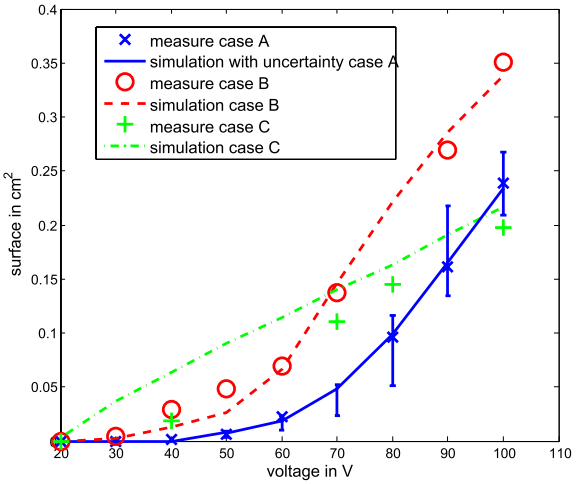

Fig. 4. Comparison for the surface of the necrosis area (curves = simulations, spots = experiments). Error bars (case A only) are computed in Section III-E.

to the shape of electropermeabilized regions computed in our simulations.

In order to provide more quantitative results, the surface of the necrosis area has been estimated from the pictures shown in Fig. 2 by using the software ImageJ [7]. Each image was converted to a 8 bit white/black image, a threshold was applied in order to delimit the EP area and the surface of which was measured. In our simulations, the surface of the necrosis area was computed based on the criterion: $\sigma_{\text{pot}} \geq \sigma_{\text{thr}} = (\sigma_0 + \sigma_1)/2$. Fig. 4 shows the obtained results and one can observe that the numerical and experimental data have the same trend, except for case C. One of the reasons may be that the positioning of the electrodes in the sample is made with a tolerance of $\sim$1 mm; this is likely to be more critical for the case C, where one electrode is dropped into the sample at only 2 mm from the edge.

E. Effect of Uncertainties

The modeling proposed in the previous section is not deeply thorough. There are some approximations in the fitting of the parameters in Ohm's law, the relation between the thresholds for the necrosis area (set experimentally in terms of darkening and numerically in terms of conductivity) is not clear and finally the positioning of the electrode is made up to a tolerance of 1 mm. The effect of these uncertainties is investigated hereafter.

Concerning Ohm's law, there are five free parameters; however, only four of them are independent, since the solution $\mathbf{v}$ of (2) is unchanged when the different conductivities are scaled by an arbitrary factor. Consequently, we define two coefficients α_1 and α_{gel}, such that $\sigma_1 = \alpha_1\sigma_0$ and $\sigma_{\text{gel}} = \alpha_{\text{gel}}\sigma_0$. Then, uncertainty is modeled by assuming that those coefficients α_1 and α_{gel}, as well as E_{thr} and k, are uniformly distributed random variables. The range of these variables is chosen $\pm 5\%$ around their mean value, that is, $\alpha_1 = 3 \pm 0.15$, $\alpha_{\text{gel}} = 20 \pm 1$, $E_{\text{thr}} = 115 \pm 5.75$ V/cm, and $k = 0.04 \pm 0.002$ cm/V. In the same way, uncertainty in the choice of the threshold for the determination of the necrosis area in simulations is dealt by introducing a random uniform variable: $\alpha_{\text{thr}} = 0.5 \pm 0.025$, such that the conductivity threshold is expressed by $\sigma_{\text{thr}} = \sigma_0 + \alpha_{\text{thr}}(\sigma_1 - \sigma_0)$. Finally, the imprecision in the positioning of the electrodes is numerically modeled by introducing two uniform random variables: $x = \pm 1$ mm and $y = \pm 1$ mm, that give the difference between the 2-D coordinates for the real and theoretical position of one of the electrodes.

Due to those random parameters, the calculated necrosis area A is a random variable which distribution is not necessary uniform. A collocation stochastic method is used to compute the probability density function $f_A(\tau)$ defined for $\tau \geq 0$. Compared with Monte Carlo methods, this technique has the advantage to extract the probabilistic information by using a few samples of the deterministic problem (around two hundred, compared with tenths of thousands for a Monte Carlo simulation).

For a sake of simplicity, we propose to show the confidence interval (CI) instead of the probability density function. In the case of a normal distribution, one can define CI $= [\bar{A} - \sigma_A, \bar{A} + \sigma_A]$, where $\bar{A}$ is the mean value and σ_A is the standard deviation; in particular, $\int_{\bar{A}-\sigma_A}^{\bar{A}+\sigma_A} f_A(\tau)d\tau = 0.68$, which means that the probability for a sample to be included in the CI is 68%. When the distribution is not normal and even not symmetric, CI can be defined in a similar way: CI $= [\bar{A} - \sigma_{A_{\text{down}}}, \bar{A} + \sigma_{A_{\text{up}}}]$, where $\sigma_{A_{\text{down}}}$ and $\sigma_{A_{\text{up}}}$ are computed such that $\int_{\bar{A}-\sigma_{A_{\text{down}}}}^{\bar{A}+\sigma_{A_{\text{up}}}} f_A(\tau)d\tau = 0.68$.

This approach has been applied for the nine voltages in case A. The error bars of Fig. 4 represent the computed CI; it can be observed that the experimental points lie within the CI. This fact supports the hypothesis that our modeling sounds realistic. However, there is a large dispersion of the uncertainties in the model; for example, at 80 V, the CI spans from -47% to $+17\%$ with respect of the mean value $\bar{A}$, which is very high compared with the considered uncertainty of the parameters ($\pm 5\%$).

F. Sensitivity

In order to explain this result, a sensitive study can be led; apart from the probability distribution $f_A(\tau)$, the stochastic method enables to extract the variance Var(A) and the contribution of each random parameter to this variance. Two quantities can be analyzed: 1) the partial variance PV and 2) the total effect variance TEV [8]. Consider for example the parameter α_1. The PV for this parameter is defined by Var$(\text{Esp}[A|\alpha_1])/\text{Var}(A)$, where Esp is the expectation operator; PV gives the relative contribution of α_1 to the variance. The TEV is defined by $1 - \text{Var}(\text{Esp}[A|-\alpha_1])/\text{Var}(A)$ where Esp$[A|-\alpha_1]$ is the conditional expectation with respect of all random variables except α_1; TEV gives the relative contribution to the variance of α_1 alone (i.e., PV) plus the contribution due to the interaction of α_1 with all the other random variables.

Results are reported in Table I. It appears that the uncertainty in the surface of the necrosis is mainly due to the position of the electrodes (PV $= 30.71\%$ for x and PV $= 28.65\%$ for y); this is not surprising since it modifies the electric field

TABLE I
PV AND TEV OF THE DIFFERENT PARAMETERS IN THE CALCULATION OF THE NECROSIS AREA AT 60 V

Quantity	α_1	α_{gel}	E_{thr}	k	α_{thr}	x	y
PV (%)	0.29	0.00	17.73	0.53	2.83	30.71	28.65
TEV (%)	0.29	0.00	24.32	3.61	6.44	43.53	41.66

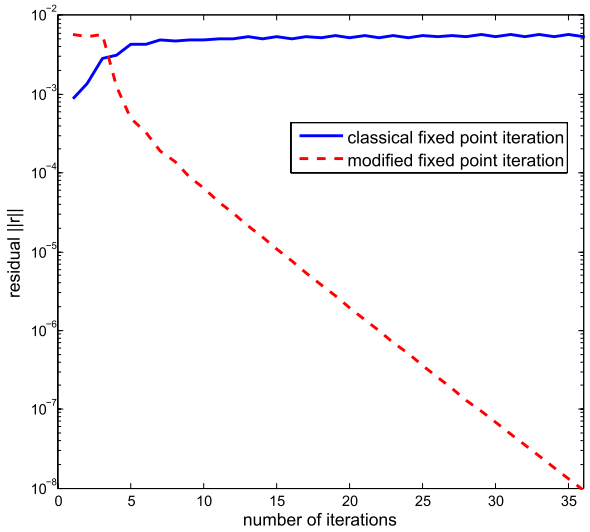

Fig. 5. Convergence study using the classical fixed point iteration and the modified one to solve the non-linear problem (3) given in case A for a voltage of 70 V.

for a given voltage. The threshold E_{thr} (PV $= 17.73\%$) is also important. In addition, there is a relation between those three variables, which is corroborated by the difference between TEV and PV. The threshold α_{thr} used to delimit the necrosis area is not so crucial as expected (TEV $= 6.44\%$). The other parameters in the building of Ohm's law are not important; this observation is favorable since the identification of those parameters in Section III-C was approximative.

IV. CONCLUSION

The experimental observation of the necrosis areas after EP on samples of potato is used to fit a model of EP based on a non-linear Ohm's law. When some uncertainties inherent to the problem are taken into account, it appears that numerical and experimental results agree for different applied voltages and positions of electrodes. In addition, the sensitivity analysis demonstrates that the most critical parameter in this model is the electric field threshold E_{thr} over which EP occurs. A limit of our model is that it is derived from a steady-state current equation; consequently, the dynamic behavior of EP is not taken into account. In particular, the value of the estimated parameters are valid only for the configuration considered in this paper (a pulse of a few milliseconds); other situations (for example application of several microseconds pulses) would most probably require another set of parameters for Ohm's law. To remove this limitation, the next step is to combine in the modeling the conductive and dielectric features of the tissue.

Algorithm 1 Resolution of the Non-Linear System Using a Modified Fixed Point Method.

solve $\mathbf{A(0)v} = \mathbf{b}$
$\|\mathbf{r_{old}}\| = +\infty$
$K = 1$
while $\|\mathbf{r_{old}}\| > tol$ **do**
  $\mathbf{r} = \mathbf{b} - \mathbf{A}(\mathbf{v})\,\mathbf{v}$
  solve $\mathbf{A}(\mathbf{v})\,\delta\mathbf{v} = \mathbf{r}$
  if $\|\mathbf{r}\| > \|\mathbf{r_{old}}\|$ **then**
    $K = K/2$
  end if
  $\mathbf{v} = \mathbf{v} + K\delta\mathbf{v}$
  $\|\mathbf{r_{old}}\| = \|\mathbf{r}\|$
end while

APPENDIX
ALGORITHM DERIVED FROM THE FIXED POINT ITERATION TO SOLVE THE NON-LINEAR PROBLEM GIVEN IN (3)

The fixed point iteration is one of the most simple method to solve a non-linear problem.

In the classical approach, the search direction $K\delta\mathbf{v}$ (Algorithm 1) is built using $K = 1$ for any iteration but this technique is not efficient in our problem as shown in Fig. 5. In the modified approach, the size of the step $K\delta\mathbf{v}$ can be reduced in order to decrease the size of the non-linear residual. This correction improves dramatically the convergence of the numerical problem (Fig. 5).

ACKNOWLEDGMENT

This work was supported in part by the MEMOVE Project under Grant ANR-BS01 006 01, in part by the Physics, Radiobiology, Medical Imaging, and Simulation Laboratory of Excellence Project under Grant ANR-11-LABX-0063, and in part by IdEx Bordeaux-CPU Project under Grant ANR-10-IDEX-03-02.

REFERENCES

[1] D. Miklavčič, B. Mali, B. Kos, R. Heller, and G. Serša, "Electrochemotherapy: From the drawing board into medical practice," *Biomed. Eng. OnLine*, vol. 13, no. 1, p. 29, 2014.
[2] D. Sel, D. Cukjati, D. Batiuskaite, T. Slivnik, L. M. Mir, and D. Miklavcic, "Sequential finite element model of tissue electropermeabilization," *IEEE Trans. Biomed. Eng.*, vol. 52, no. 5, pp. 816–827, May 2005.
[3] O. Kavian, M. Leguèbe, C. Poignard, and L. Weynans, "'Classical' electropermeabilization modeling at the cell scale," *J. Math. Biol.*, vol. 68, nos. 1–2, pp. 235–265, Dec. 2012.
[4] C. T. Kelley, *Iterative Methods for Linear and Nonlinear Equations*. Philadelphia, PA, USA: SIAM, 1995.
[5] A. Silve, "Nouveaux dispositifs pour l'application contrôlée d'impulsions électriques nanosecondes et pour la détection de leurs effets sur les cellules. Nouveaux résultats et hypothèses sur les paramètres contrôlant l'électroperméabilisation des cellules biologiques," Ph.D. dissertation, Dept. Biopharmaceuticals Technol., Univ. Paris Sud, Paris, France, 2011.
[6] D. Voyer, F. Musy, L. Nicolas, and R. Perrussel, "Comparison of methods for modeling uncertainties in a 2D hyperthermia problem," *Prog. Electromagn. Res.*, vol. 11, pp. 189–204, 2009.
[7] *Software ImageJ*. [Online]. Available: http://rsbweb.nih.gov/ij/, accessed Jan. 2014.
[8] I. M. Sobol, "Sensitivity estimates for nonlinear mathematical models," *Math. Modelling Comput. Experiments*, vol. 1, no. 4, pp. 407–414, 1993.